Am J Physiol Renal Physiol 306: F430–F441, 2014.
First published November 27, 2013; doi:10.1152/ajprenal.00720.2012.

Basic fibroblast growth factor reduces functional and structural damage in chronic kidney disease

Sandra Villanueva,[1] Felipe Contreras,[1] Andrés Tapia,[1] Juan E. Carreño,[1] Cesar Vergara,[1] Ernesto Ewertz,[1] Carlos Cespedes,[2] Carlos Irarrazabal,[1] Mauricio Sandoval,[1] Victoria Velarde,[2] and Carlos P. Vio[2]

[1]*Laboratory of Integrative and Molecular Physiology, Los Andes University, Santiago, Chile; and* [2]*Department of Physiology, Center for Aging and Regeneration, Pontificia Universidad Católica de Chile, Santiago, Chile*

Submitted 27 December 2012; accepted in final form 26 November 2013

Villanueva S, Contreras F, Tapia A, Carreño JE, Vergara C, Ewertz E, Cespedes C, Irarrazabal C, Sandoval M, Velarde V, Vio CP. Basic fibroblast growth factor reduces functional and structural damage in chronic kidney disease. *Am J Physiol Renal Physiol* 306: F430–F441, 2014. First published November 27, 2013; doi:10.1152/ajprenal.00720.2012.—Chronic kidney disease (CKD) is characterized by loss of renal function. The pathological processes involved in the progression of this condition are already known, but the molecular mechanisms have not been completely explained. Recent reports have shown the intrinsic capacity of the kidney to undergo repair after acute injury through the reexpression of repairing proteins (Villanueva S, Cespedes C, Vio CP. *Am J Physiol Regul Integr Comp Physiol* 290: R861–R870, 2006). Stimulation with basic fibroblast growth factor (bFGF) could accelerate this process. However, it is not known whether bFGF can induce this phenomenon in kidney cells affected by CKD. Our aim was to study the evolution of renal damage in animals with CKD treated with bFGF and to relate the amount of repairing proteins with renal damage progression. Male Sprague-Dawley rats were subjected to ⅚ nephrectomy (NPX) and treated with bFGF (30 μg/kg, NPX+bFGF); a control NPX group was treated with saline (NPX+S). Animals were euthanized 35 days after bFGF administration. Functional effects were assessed based on serum creatinine levels; morphological damage was assessed by the presence of macrophages (ED-1), interstitial α-smooth muscle actin (α-SMA), and interstitial collagen through Sirius red staining. The angiogenic factors VEGF and Tie-2 and the epithelial/tubular factors Ncam, bFGF, Pax-2, bone morphogenic protein-7, Noggin, Lim-1, Wnt-4, and Smads were analyzed. Renal stem cells were evaluated by Oct-4. We observed a significant reduction in serum creatinine levels, ED-1, α-SMA, and Sirius red as well as an important induction of Oct-4, angiogenic factors, and repairing proteins in NPX+bFGF animals compared with NPX+S animals. These results open new perspectives toward reducing damage progression in CKD.

chronic kidney disease; bFGF; renal recovery

CHRONIC KIDNEY DISEASE (CKD) is a clinical condition that results in the progressive loss of kidney function to a terminal stage (18). Independent of its multiple etiologies, the disease concludes with similar morphological characteristics, namely, tubular fibrosis and glomerular sclerosis. Both conditions induce the progressive destruction of nephrons and irreversible kidney function failure.

CKD is a worldwide public health problem, due to its continuous increase in prevalence and incidence (9), the high cost of its treatment, and poor prognosis for patients. Many therapies have been developed in an attempt to reduce the progression of tissue damage in CKD, such as angiotensin I-converting enzyme inhibitors and angiotensin II receptor antagonists (14, 31, 33, 38, 43). Nonetheless, they have not shown significant improvements in glomerular filtration rates (GFR) or tubular function that could prevent the end stage of renal disease (ESRD) (33). Thus research for new alternative treatments in CKD is one of the primary concerns in nephrology.

Acute renal failure (ARF), contrary to CKD, has a regeneration phase (3), characterized by increases in GFR, decreases in serum creatinine levels, and the recovery of the damaged tissue (45). Our results, obtained from the regeneration phase of ischemic ARF suggest that the expression of repairing proteins involved in renal epithelium and tubule formation during renal development are potentially essential for the regeneration process (49). These proteins include mesenchymal factors [i.e., neural cell adhesion molecules (Ncam) (1), Wilms' tumor 1 (WT-1) (54), and vimentin (55)]; epithelial proteins [i.e., paired homeobox-2 (Pax-2) (41), basic fibroblast growth factor (bFGF) (20), and zona occludens-1 (ZO-1);] and tubular proteins [i.e., Lim-1, Wnt-4 and Engrailed (34)]. This group also includes bone morphogenic protein-7 (BMP-7) (12), its antagonist Noggin (5, 50), and the Smad transcription factors (24).

A second group of proteins involved in the formation of renal vasculature that are reexpressed after renal damage consist of angiogenic factors. One of them is the vascular endothelial growth factor (VEGF), which is essential in endothelial and glomerular development (4). Its expression is maintained in the adult kidney at the glomeruli, where it preserves the glomerular filtration barrier. Recent studies have shown that VEGF has a protective role against glomerular damage (21), and its expression has been correlated with the degree of glomerular sclerosis (30). Another angiogenic protein, namely, the angiopoietin receptor Tie-2, is known to be expressed in late mature stages of the mouse metanephros, when interstitial and glomerular capillaries begin to form. It has been observed to play a crucial role in maintaining vascular integrity (23, 35) and in the regeneration phase of ARF (49).

bFGF is a protein secreted by the ureteric bud, and it is necessary for the induction of cellular aggregation (20, 24). The main effects of bFGF are inhibition of apoptosis (2), stimulation of epithelial condensation, and maintenance of WT-1 synthesis (a transcription factor that induces the transformation of mesenchymal cells into metanephric tissue) (25). bFGF is not present in tubular cells in adult kidneys, but it is reexpressed in response to damage induced by ARF (49). Moreover, bFGF can induce the expression of repairing pro-

Address for reprint requests and other correspondence: S. Villanueva, Laboratorio de Fisiología Integrativa y Molecular, Universidad de los Andes, San Carlos de Apoquindo 2200, Santiago, Chile (e-mail: svillanueva@uandes.cl).

teins and accelerate the tissue repair process when it is exogenously added (48) or, on the contrary, renal damage could be prolonged when it is inhibited (47). In the latter case, kidney cells could be induced to an undifferentiated state, where their mitotic capabilities could be recovered. In addition, it has been reported that bFGF improves the proliferation rate of kidney cells, maintaining potential differentiation in mesenchymal stem cells (MSC) in vitro (8). Based on this, we studied additional effects of bFGF on renal stem cells (SC).

Our hypothesis sustains the idea that bFGF can induce kidney cells to reexpress repairing factors in CKD. This treatment should delay the damage progression caused by CKD. We performed a structural and functional analysis after bFGF injection in rats subjected to ⅝ nephrectomy (NPX) so as to relate the presence of repairing proteins with the progression of CKD.

MATERIALS AND METHODS

Animals. Adult male Sprague-Dawley rats (220–250 g, n = 7/group) were housed in a 12:12-h light-dark cycle and maintained at the University of Los Andes animal care facilities. Food and water were supplied ad libitum. The treated (NPX with bFGF injection) and control (NPX with saline) animals were weighed at the beginning and end of each experiment. All experimental procedures were in accordance with institutional and international standards for the humane care and use of laboratory animals (Animal Welfare Assurance Publication A5427-01, Office for Protection from Research Risks, Division of Animal Welfare, National Institutes of Health).

NPX and treatment with bFGF. We used an established model of chronic damage that resembles the structural and functional changes that take place in CKD (13). The animals were anesthetized with ketamine:xylazine (25:2.5 mg/kg ip). The left kidney was exposed by a retroabdominal incision, and renal irrigation was reduced by clamping two branches of the renal artery. Then, the incisions were sutured in the muscular layer and skin. Rats were allowed to recover in a warm room with water and food ad libitum. After 1 wk, another incision was made and the right kidney was removed. At this moment, a single dose of bFGF (30 μg/kg; 233-FB-025, R&D System) (46, 48) in a total volume of 200 μl was injected into the renal arteries of the remaining kidneys of the animals in the treated group. Saline (NPX+S) was injected into the kidneys of animals in the control group. Rats were euthanized under anesthesia (ketamine:xylazine) 35 days after the last surgery, and the remaining kidneys were removed and processed for Western blotting (WB) and immunohistochemistry (IHC) analyses.

Determination of functional and tissue damage. As described before (49), functional damage was analyzed based on serum creatinine levels (Beckman creatinine analyzer 2). At the moment of death, blood samples were obtained from the inferior cava vein. Histological damage was evaluated through periodic acid-Schiff (PAS) staining and by immunolocalization of macrophages (ED-1) and interstitial α-smooth muscle actin (α-SMA), which were used as markers of tissue damage. Total collagen content was detected by staining with Sirius red.

Kidney interstitial injury was graded (0–5) in a blinded manner on the basis of tubular dilation and protein casts as follows: 0, no changes present; *grade 1*, 10% changes present; *grade 2*, 10–25% involvement; *grade 3*, 25–50%; grade 4, 50–75%; and grade 5, 75–100%. For each biopsy, the entire cortical and outer medullary regions were evaluated (15–30 fields of 1 mm^2), and a mean score per biopsy was calculated.

Tissue processing and immunohistochemical analysis. Immunohistochemical studies in Paraplast-embedded sections were performed as previously described (47–49, 51). Immunolocalization studies were performed by using an indirect immunoperoxidase technique (51). Briefly, tissue sections were incubated with primary antibody overnight at room temperature, followed by incubation with the corresponding secondary antibody and the peroxidase-antiperoxidase complex. Peroxidase activity was detected by incubation with 0.1% (wt/vol) 3,3′-diaminobenzidine and 0.03% (vol/vol) hydrogen peroxide. For some specific antibodies, immunoreactivity was revealed by using a secondary antibody conjugated to alkaline phosphatase in the presence of nitro-blue tetrazolium/5-bromo-4-chloro-3-indolyl-phosphate (NBT:BCIP, 4.5:3.5 μl/ml) in buffer (Tris 100 mM; pH 9.5). Controls for the immunostaining procedure were prepared by omitting the first antibody and replacing it with normal or preimmune serum of the same species (52).

Each immunoreactive area per field was determined by image analysis using Simple PCI software from Compix Imaging Systems (Cranberry Township, PA). Total immunostained (brown) cells were averaged and expressed as the average absolute values or the average percentage of each stained cell area per field as previously described (52) with minor modifications.

Antibodies and chemicals. The primary antibodies that were used were the same antibodies recently used by us (47–49), namely, monoclonal antibodies against Lim 1+2 (clone 4F2), vimentin (clone 40E-C), and Ncam (clone 5B8). They were obtained from the Developmental Studies Hybridoma Bank, developed under the sponsorship of the Eunice Kennedy Shriver National Institute of Child Health and Human Development and maintained by the Department of Biological Sciences at the University of Iowa (Iowa City, IA). Goat polyclonal antibodies against Pax-2, BMP-7, Smads 1-5-8, Smads 2–3, as well as rabbit polyclonal antibodies against Tie-2, bFGF, and the monoclonal antibody against VEGF (clone C-1) were provided by Santa Cruz Biotechnology (Santa Cruz, CA). The presence of SC was determined by measuring protein expression of Oct-4 from Santa Cruz Biotechnology. Monoclonal antibodies against macrophages (clone ED-1) were obtained from Biosource (Camarillo, CA), α-SMA (clone 1A4) was from Sigma-Aldrich (St. Louis, MO), and the monoclonal antibody against Noggin was a gift from Dr. R. Harland. The presence of SC was determined using an anti-Oct-4 (octamer-binding protein-4) antibody (Santa Cruz Biotechnology) and an anti-CD73 antibody (R&D Systems). The monoclonal antibody against hypoxia-induced factor 1α (HIF-1α; clone H1α67) was provided by Novus Biological (Littleton, CO). Finally, the polyclonal antibody against α-tubulin (11H10) was obtained from Cell Signaling (Boston, MA).

Secondary antibodies and the corresponding peroxidase-antiperoxidase complexes were purchased from MP Biomedicals, (Aurora, OH). Triton X-100, DAB, NBT:BCIP, carrageenan, Tris·HCl, hydrogen peroxide, phosphate salts, and other chemicals were purchased from Sigma-Aldrich.

IB. Whole kidney sections (~1 mm thick) were homogenized, and protein concentration was determined as previously described (49). WB was performed as we described previously (47–49). For SDS-PAGE, proteins were mixed with sample buffer (100 mM Tris·HCl, pH 6.8, 200 mM dithiothreitol, 4% SDS, 0.2% bromophenol blue, 20% glycerol), transferred to nitrocellulose membranes, and blocked as previously described (49). After blocking, membranes were probed with the corresponding antibody, washed with Tris-buffered saline and Tween 20 (TBS-T), and incubated with horseradish peroxidase (HRP) conjugated to the secondary antibody for 1 h at room temperature. Immunoreactivity was detected by using the enhanced chemiluminescence technique with reagents obtained from PerkinElmer Life Sciences (Boston, MA).

Blots were scanned, and densitometric analysis was performed by using the public domain National Institutes of Health Image program v1.61 (US NIH, http://rsb.info.nih.gov/nih-image). Expression of α-tubulin was used to correct for variation in sample loading.

Detection and quantification of renal cell apoptosis by in situ end labeling of fragmented DNA (terminal transferase-dUTP-nick-end labeling method) and caspase-3 detection. Apoptotic cells in kidney tissue slices were visualized using an Apop Tag Fluorescein In Situ

Table 1. *Renal damage indices: comparison of renal morphology in the nephrectomy (NPX) model treated with basic fibroblast growth factor (NPX+bFGF) or saline (NPX+S) 35 days after induced damage*

	ED-1, μm^2	α-SMA, μm^2	Sirius red, μm^2	DT (score 0–5)	PC (score 0–5)
NPX+S (n = 7)	5.98 ± 0.32	4.43 ± 0.51	12.78 ± 0.62	4.7 ± 0.7	5.3 ± 0.9
NPX+ bFGF (n = 7)	2.21 ± 0.11*	1.28 ± 0.04*	4.11 ± 0.26*	1.9 ± 0.8*	1.0 ± 0.4*

Values are average ± SE. ED-1, macrophage abundance; α-SMA, interstitial α-smooth muscle actin; Sirius red, fibrosis; DT, dilated tubules; PC, protein casts. *$P < 0.05$ vs. NPX+S.

Apoptosis Detection Kit by means of the indirect terminal transferase-dUTP-nick-end labeling (TUNEL) method from Chemicon (Temecula, CA), following the manufacturer's protocol. Paraffin-embedded tissue sections were dewaxed, rehydrated, and permeabilized with proteinase K (20 μg/ml) for 15 min, incubated with equilibration buffer for 5 min, and with tdt enzyme for 60 min. The reaction was finished with a 10-min stop/wash buffer. Sections were incubated with an anti-digoxigenin conjugate for 30 min at room temperature, washed in PBS, and blocked with PBS/BSA for 60 min, after which they were incubated with an anti-caspase-3 antibody acquired from Promega (Madison, WI) at 4°C for 12 h. The sections were incubated with a green fluophore (Alexa 488) polymer conjugated to goat anti-rabbit Ig, which was obtained from Molecular Probes (Eugene, OR). Immunoreactive fluorescein was visualized by using VECTASHIELDS+DAPI (catalog no. H-1200, Vector Laboratories, Burlingame, CA) as the substrate to stain nuclei, and adding 1 drop of anti-Fade solution (i.e., catalog no. S7461, Molecular Probes). Fluorescence was viewed by microscopy with appropriate excitation and emission filters.

Statistical analysis. Differences were assessed with the nonparametric Mann-Whitney *U*-test for pairwise comparisons when overall significance was detected. The significance level was $P < 0.05$. The analysis in Table 1 was done by using Student's *t*-test, with a significance level of $P < 0.05$.

RESULTS

Determination of functional damage. Functional damage induced by NPX was verified based on serum creatinine levels. Nephrectomized rats treated with saline solution (NPX+S) had higher serum creatinine levels (1.03 ± 0.15 mg/dl) after 35 days of nephrectomy. Interestingly, serum creatinine values observed in NPX animals treated with bFGF (NPX+bFGF) significantly decreased when measured 35 days after injections (0.46 ± 0.16 mg/dl; $P < 0.05$).

Determination of tissue damage. Histological tissue damage was evaluated by PAS staining and by the presence of renal damage markers (ED-1 and α-SMA) and the fibrosis marker Sirius red in kidney sections analyzed 35 days after nephrectomy. Sections from NPX+S kidneys showed morphological alterations that are characteristic of chronic damage, such as loss of brush border, flattening of the epithelia, presence of tubular detritus, and a large quantity of dilated tubules (Fig. 1*A*). NPX+bFGF kidneys showed conserved morphologies, but with important amounts of cellular mitosis (Fig. 1*E*).

Additionally, these parameters were quantified, based on the levels of dilated tubules (DTs), protein casts (PCs), macrophage abundance (ED-1), interstitial α-SMA, and Sirius red. The quantifications of these parameters are shown in Table 1.

Increases in the presence of macrophages ED-1 (5.98 ± 0.32 μm^2), interstitial α-SMA (4.43 ± 0.51 μm^2), and Sirius red (12.78 ± 0.62 μm^2) were observed in NPX+S animals 35 days postnephrectomy (Fig. 1, *B–D*), which were similar to what had been previously published by the present research group. bFGF administration (NPX+bFGF) to the kidneys resulted in lower staining for these markers (2.21 ± 0.17 μm^2 for ED-1, 1.28 ± 0.04 μm^2 for α-SMA, and 4.11 ± 0.26 μm^2 for Sirius red) (Fig. 1, *F–H*), indicating lower degrees of damage in this condition ($P < 0.05$). Immunostaining controls were made by omitting the first antibody and replacing it with normal or preimmune serum of the same species (52), in which cases positive staining was not observed (data not shown).

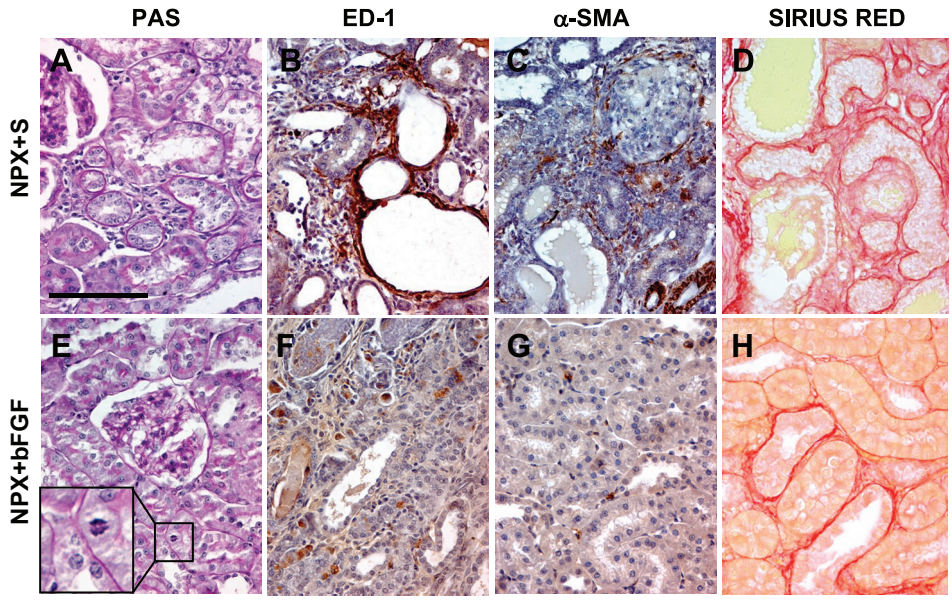

Fig. 1. Morphological damage in kidneys from rats after ⅝ nephrectomy (NPX). Immunohistochemistry was performed in kidney samples collected 35 days after NPX (n = 7/NPX group) injected with saline (S; *A–D*) or with basic fibroblast growth factor (bFGF; *E–H*). The tissue damage was evaluated by periodic acid-Schiff (PAS) staining (*A* and *E*; *inset* indicates cells in mitosis); renal damage markers such as ED-1 for detecting the presence of macrophages (*B* and *F*), or α-smooth muscle actin (SMA) for detecting the presence of myofibroblasts (*C* and *G*). Fibrosis was evaluated by Sirius red staining (*D* and *H*). Staining for ED-1 and α-SMA was performed using peroxidase and was revealed with diaminobenzidine (DAB; brown color reaction). Scale bar = 100 μm.

Detection of angiogenic markers HIF-1α, VEGF, and Tie-2 in kidneys during CKD. Nuclear transcription factor HIF-1α was higher in the remaining kidney of NPX animals treated with bFGF compared with NPX animals 35 days after surgery, as observed by Western blotting and immunohistochemistry (Figs. 2*A* and 3, *A* and *B*) ($P < 0.05$). Staining for this factor was observed mainly in the papillary collecting tubules, thick ascending limbs, and proximal tubular cells, localized mainly in the renal inner and outer medulla, as described previously, and was not modified by treatment with bFGF (48, 49). Immunostaining controls were made by omitting the first antibody and replacing it with normal or preimmune serum from the same species (52), in which cases positive staining was not observed (data not shown).

VEGF and Tie-2 are markers induced by hypoxia, which promote the expression of angiogenic factors. In this study, we observed lower levels of both proteins analyzed by WB in NPX+S kidneys [1.26 ± 0.15 densitometry units (DU) for VEGF and 0.84 ± 0.09 DU for Tie-2] 35 days post-NPX compared with NPX+bFGF kidneys (6.03 ± 0.45 DU for VEGF and 8.93 ± 1.39 DU for Tie-2) ($P < 0.05$) (Fig. 2, *B* and *C*). These results were verified by IHQ (Fig. 3, *C* and *D* and *E* and *F*). Both proteins were localized in proximal tubule cells, from the outer medulla, as described previously, without modifications in localization after treatment (4, 21, 23).

Expression of mesenchymal, epithelial, and tubular markers in the remnant kidney of NPX animals. Representative expression patterns for mesenchymal (Ncam), epithelial (bFGF, Pax-2), and tubular markers (Lim-1, Wnt-4) 35 days post-NPX are shown in kidneys treated with saline or bFGF. In NPX+bFGF kidneys, we observed increased levels of Ncam, bFGF, and Pax-2 (1.83 ± 0.28, 3.25 ± 0.80, and 2.10 ± 0.30 DU, respectively) compared with NPX+S (0.85 ± 0.09 DU for Ncam; 0.68 ± 0.18 DU for bFGF, and 0.67 ± 0.20 DU for Pax-2) ($P < 0.05$) (Fig. 4, *A–C*).

These results were confirmed by IHC for bFGF and Pax-2 (Fig. 5, *A–D*), which were localized mainly in the proximal tubules of the outer medulla (6). Staining for both markers was higher in kidneys injected with bFGF (*B* and *D*) vs. kidneys injected with saline (*A* and *C*).

Similar patterns were observed with the tubular markers Lim-1 and Wnt-4; that is, both markers were highly expressed in NPX+bFGF animals (3.39 ± 0.81 DU for Lim-1 and 2.48 ± 0.43 DU for Wnt-4) compared with NPX+S (1.26 ± 0.15 DU for Lim-1 and 0.86 ± 0.08 DU for Wnt-4) (Fig. 6, *A* and *B*).

BMP-7, a survival factor for undifferentiated mesenchyme (11), is antagonized by Noggin (5, 50) and activates the transcription factors Smad 1 and 5 (24). We evaluated the levels and localizations of proteins involved in this transcription pathway 35 days after NPX in kidneys treated with bFGF or saline. In NPX+S kidneys, we observed lower levels of BMP-7 (Fig. 7*A*), Noggin (Fig. 7*B*), Smads 1-5-8 (Fig. 7*C*), and Smad 4 (Fig. 7*D*) (0.83 ± 0.09, 1.32 ± 0.18, 1.14 ± 0.08, and 0.72 ± 0.16 DU, respectively). On the other hand, a significant increase ($P < 0.05$) in the levels of these proteins was detected in NPX+bFGF (4.89 ± 1.09 DU for BMP-7, 7.51 ± 0.39 DU for Noggin, 9.85 ± 0.70 DU for Smads 1-5-8, and 3.96 ± 0.73 DU for Smad 4) compared with NPX+S ($P < 0.05$) (Fig. 7, *A–D*). These results were confirmed by IHC for BMP-7, Smads 1-5-8, and Smad 4. The remaining kidneys from NPX rats treated with saline (S) (Fig. 8, *A*, *C*, and *E*) showed less staining compared with kidneys injected with bFGF (Fig. 8, *B*, *D*, and *F*), which showed strong staining intensity. Staining for BMP-7 and Smad 4 was mainly localized in distal tubules, while expression for Smads 1-5-8 was localized in the proximal and distal tubules (Fig. 8). Immunostaining controls were made by omitting the first antibody and replacing it with normal or preimmune serum from the same species (52), in which cases positive staining was not observed (data not shown).

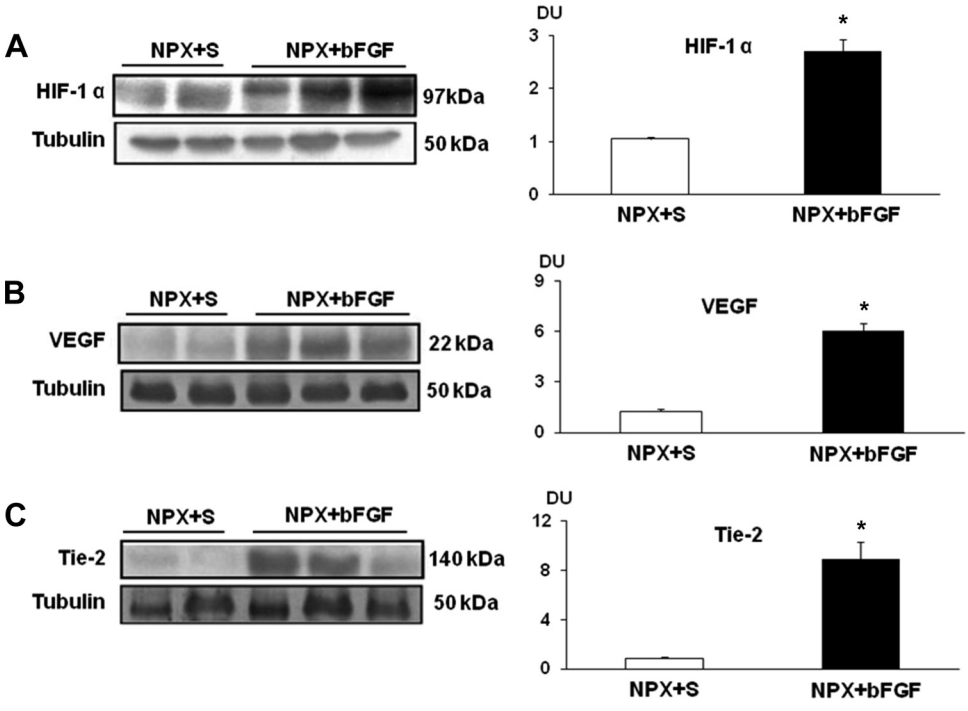

Fig. 2. Immunoblotting of endothelial cell markers in kidney recovery. The remaining kidneys from NPX rats was injected with saline (S) or bFGF and were processed for immunoblotting 35 days post-NPX using antibodies against hypoxia-induced factor (HIF)-1α (*A*), VEGF (*B*), or Tie-2 (*C*). *Right*: values are the average ± SE of 3 different kidneys. *Left*: representative pictures from blots. DU, densitometry units. Tubulin was used as loading control. *$P < 0.05$.

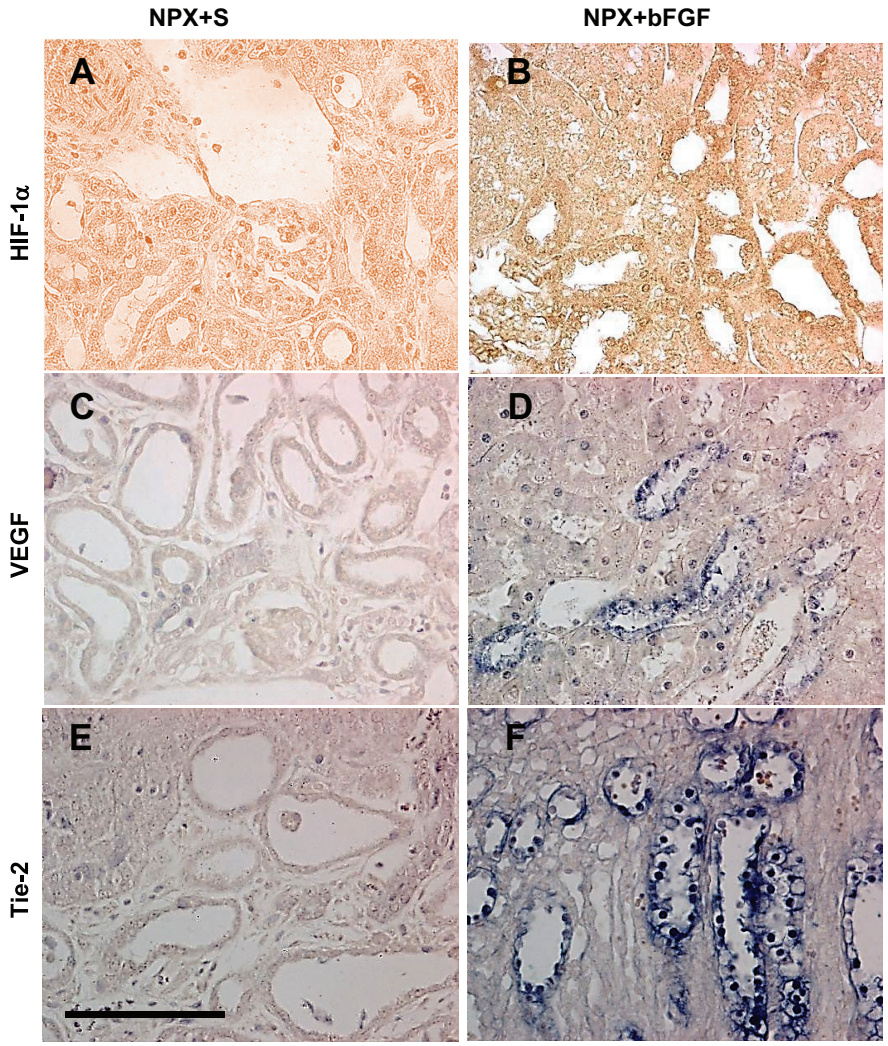

Fig. 3. Immunolocalization of endothelial cell markers in kidneys from NPX rats. Staining intensity for HIF-1α (*A* and *B*), VEGF (*C* and *D*), and Tie-2 (*E* and *F*) were observed in the remaining kidneys 35 days after NPX and injection with bFGF (*B*, *D*, and *F*) or saline (*A*, *C*, and *E*); $n = 7$/group. For HIF-1α, peroxidase activity was revealed with DAB (brown color reaction). For VEGF and Tie-2, the secondary antibody was conjugated with alkaline phosphatase and developed with NBT:BCIP (blue reaction). Scale bar = 100 μm.

In situ cell death detection and caspase-3 immunohistochemistry. TUNEL was used to detect DNA double-strand breaks. In control kidneys injected with saline, TUNEL staining was predominately localized in proximal tubule cells and some in collecting duct cells from the inner and outer medulla (Fig. 9*A*). In addition, bFGF-treated kidneys did not show any reaction to the TUNEL assays (11.21/hpf) (Fig. 9*C*). In animals injected with saline, a noticeable increase in signal, staining the whole nucleus, was observed 35 days after NPX (~32.13/hpf) (Fig. 9A). The majority of TUNEL-positive cells exhibited morphological features of apoptotic death (cytoplasm shrinkage and nucleus condensation).

To verify whether this TUNEL-positive signal was due to apoptosis, we examined caspase-3 cleavage (activation) in NPX rat kidneys with and without bFGF. Caspase-3 immunostaining was observed to dramatically increase in the inner and outer medullary areas of kidneys injected with saline 35 days after NPX (34.11/hpf) (Fig. 9*B*). The majority of caspase-3-positive cells had apoptotic morphology, and staining was predominantly present in proximal tubular cells and, to a lesser degree, in collecting duct cells. The correlation between caspase-3 and TUNEL was evident. Thus we determined a positive correlation (r: 0.62) between caspase-3 protein and TUNEL ($P < 0.05$). On the other hand, in the sample of bFGF-treated kidneys, cells showed low caspase-3 immunostaining (11.21/hpf) (Fig. 9*D*).

Renal SC detection. The presence of the renal SC marker Oct-4 was evaluated 35 days after nephrectomy. IHC staining was not observed in NPX+S animals (Fig. 10*A*; 0.4 ± 0.1 μm^2). In contrast, NPX animals injected with bFGF showed intense staining (6.40 ± 0.51 μm^2), primarily in the nuclei of tubular cells 35 days after nephrectomy (Fig. 10*B*). This difference was significant ($P < 0.05$). Oct-4 expression evaluated by WB is presented in Fig. 10*C*, where NPX+S animals are observed to present low Oct-4 expression (1.1 ± 0.3 DU). NPX+bFGF animals showed a significant increase (4.8 ± 0.8 DU) compared with the NPX+S group ($P < 0.05$). The α-tubulin total protein level was used for normalization.

To further verify the presence of stem cells in renal tissue after NPX, the presence of the marker CD73 was evaluated 35 days after nephrectomy. As observed for Oct-4, CD73 was not present in kidneys from NPX+S animals (Fig. 11, *A–C*). In contrast, CD73 not only was present in NPX+bFGF animals but colocalized with Oct-4 as well (Fig. 11, *D–F*).

DISCUSSION

Embryonic kidney development is characterized by undifferentiated cell proliferation and subsequent daughter cell differentiation into specific phenotypes (49). This phenomenon is

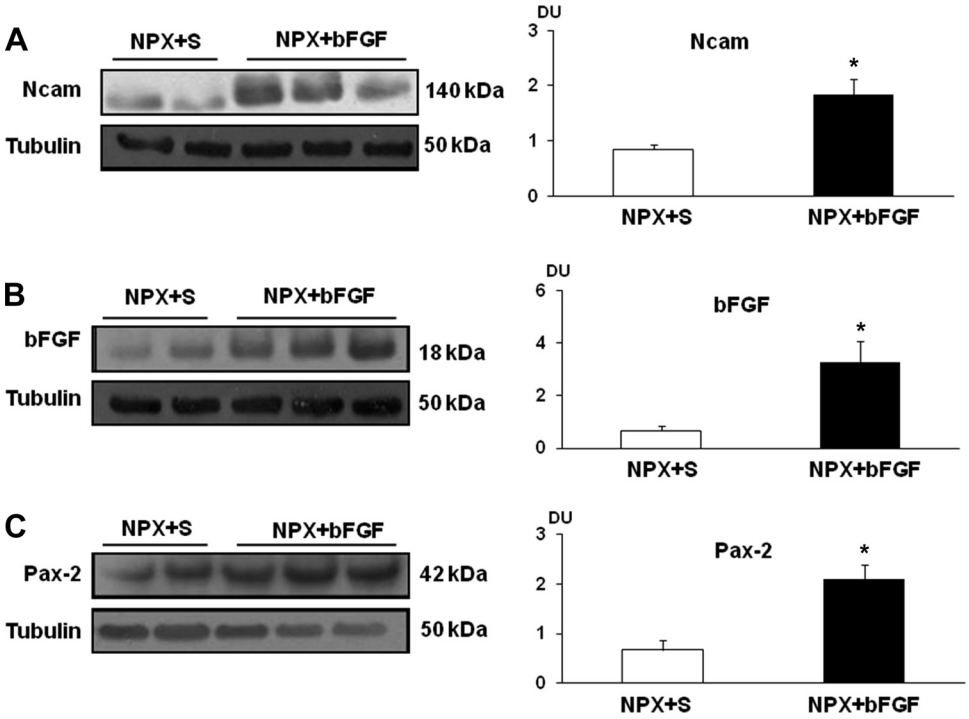

Fig. 4. Expression of early epithelial markers in NPX animals. Immunoblots (*left*) were performed for morphogenic proteins: Ncam (*A*), bFGF (*B*), and Pax-2 (*C*) 35 days after NPX. Bar graphs (*right*) represent the average ± SE of band intensity quantification in 3 different kidneys. Tubulin was used as loading control. $*P < 0.05$.

the consequence of sequential morphogenic expression that is involved in kidney fetal development. In previous reports, it has been observed that one morphogen, namely, bFGF, has a beneficial role in angiogenic factor expression (26, 27) and in myocardial infarction (46). In addition, we have demonstrated that treatment with bFGF in ARF can induce the expression of repairing proteins and, consequently, early renal regeneration (48). Studies in CKD have not addressed the potential role of morphogens in renal recovery. Therefore, in the present study we evaluated the effect of bFGF on CKD and its effect on the progression of this pathology.

We assessed the effects of bFGF 35 days after surgery, because the animals had developed all chronic renal failure markers by that time. Since we used a single bFGF injection during nephrectomy, it was possible to expect no effect after a month. Nevertheless, damage in the bFGF-injected kidneys

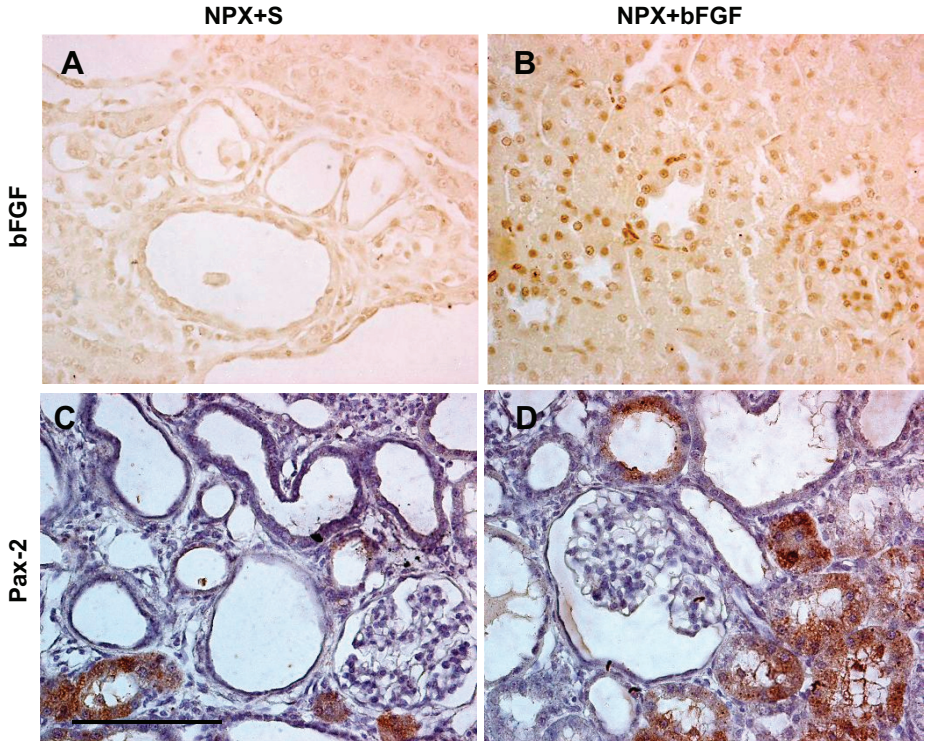

Fig. 5. Immunolocalization of early epithelial markers in kidneys from NPX rats. Kidney slices were immunostained for bFGF (*A* and *B*) and Pax-2 (*C* and *D*) 35 days after NPX and injection with bFGF (*B* and *D*) or saline (*A* and *C*); $n = 7$/group. The early epithelial proteins Pax-2 and bFGF were localized in the proximal tubular cells in the inner and outer medulla. Staining was done using peroxidase and was revealed with DAB (brown color reaction). Scale bar = 100 μm.

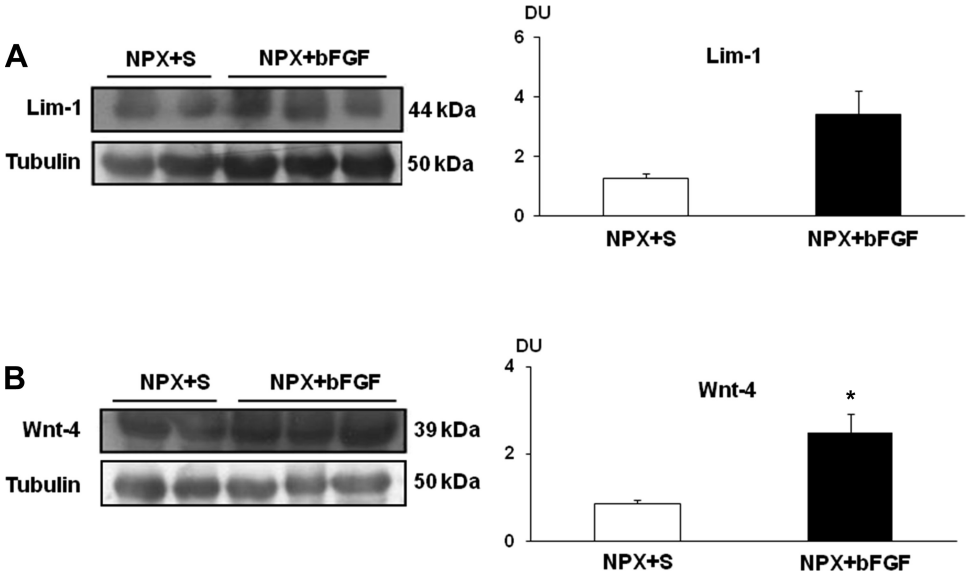

Fig. 6. Expression of tubulogenesis markers in kidneys from NPX rats. Immunoblots (*left*) were performed for Lim-1 (*A*) and Wnt-4 (*B*) 35 days after NPX and injection with saline or bFGF. Bar graphs (*right*) represent the average ± SE of band intensity quantification from 3 different kidneys. Tubulin was used as loading control. $*P < 0.05$.

was significantly lower than what was observed in the saline-injected kidneys. This could be explained by the prolonged stability of the bound growth factor.

The half-life of bFGF activity at 32°C is estimated to be 24 h (42), but bFGF binding to low-affinity receptors, which are present on the cell surface and in the basement membrane, is very stable in animal models. Indeed, in corneas with denuded epithelia, it has been shown that the bound growth factor remains biologically active at least 18 days after a single topical application (37) because, due to such binding, it is protected from proteolytic degradation (42). The prolonged half-life of the bound bFGF justifies the use of bFGF in this context and may explain why one single application of bFGF at the beginning of the experiment was sufficient to enhance the survival of renal cells (39).

Animals suffering from induced CKD, but treated with bFGF, did not show increases in serum creatinine levels (i.e., ED-1 and interstitial α-SMA) compared with nontreated animals. This suggests a reduction in renal damage or at least a delay in the progression of the disease. These results could be attributed to the role of bFGF, which can induce the expression of repairing proteins that reduce functional and morphological renal tissue damage (48). In addition, it has been reported that bFGF can induce the proliferation of renal cells (48), leading to

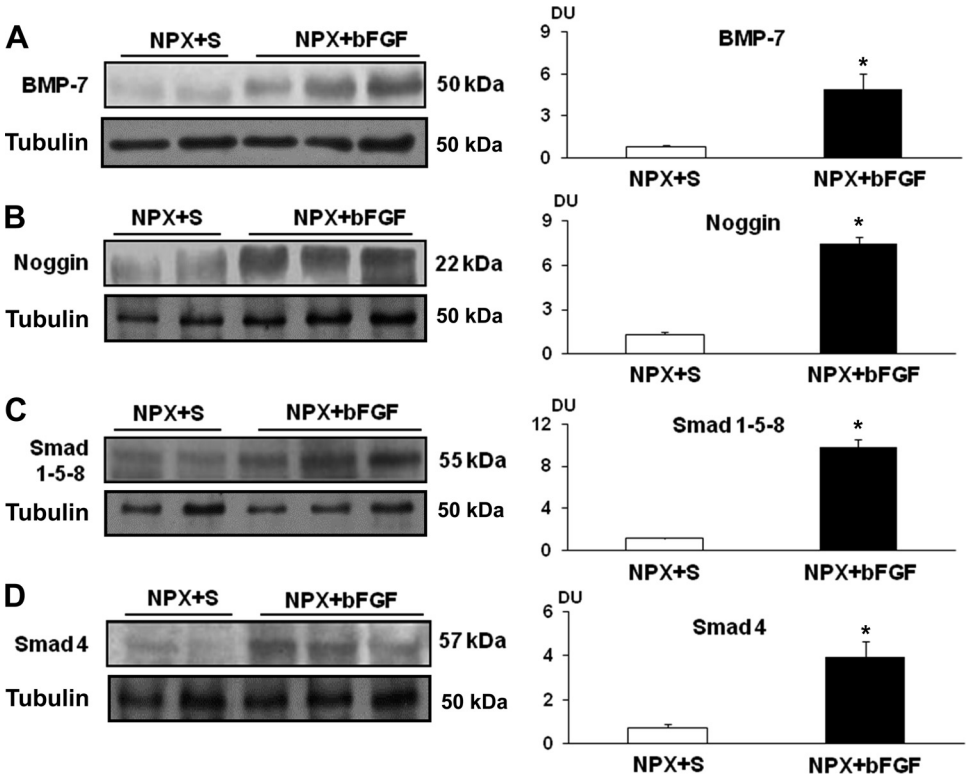

Fig. 7. Expression of the bone morphogenic protein (BMP)-7 signaling pathway in the remaining kidneys of NPX rats. Immunoblots (*left*) were performed for BMP-7 (*A*), Noggin (*B*), Smads 1-5-8 (*C*), and Smad 4 (*D*) 35 days after NPX and injection with saline or bFGF. Bar graphs (*right*) represent the average ± SE of band intensity quantification from 3 different kidneys. Tubulin was used as loading control. $*P < 0.05$.

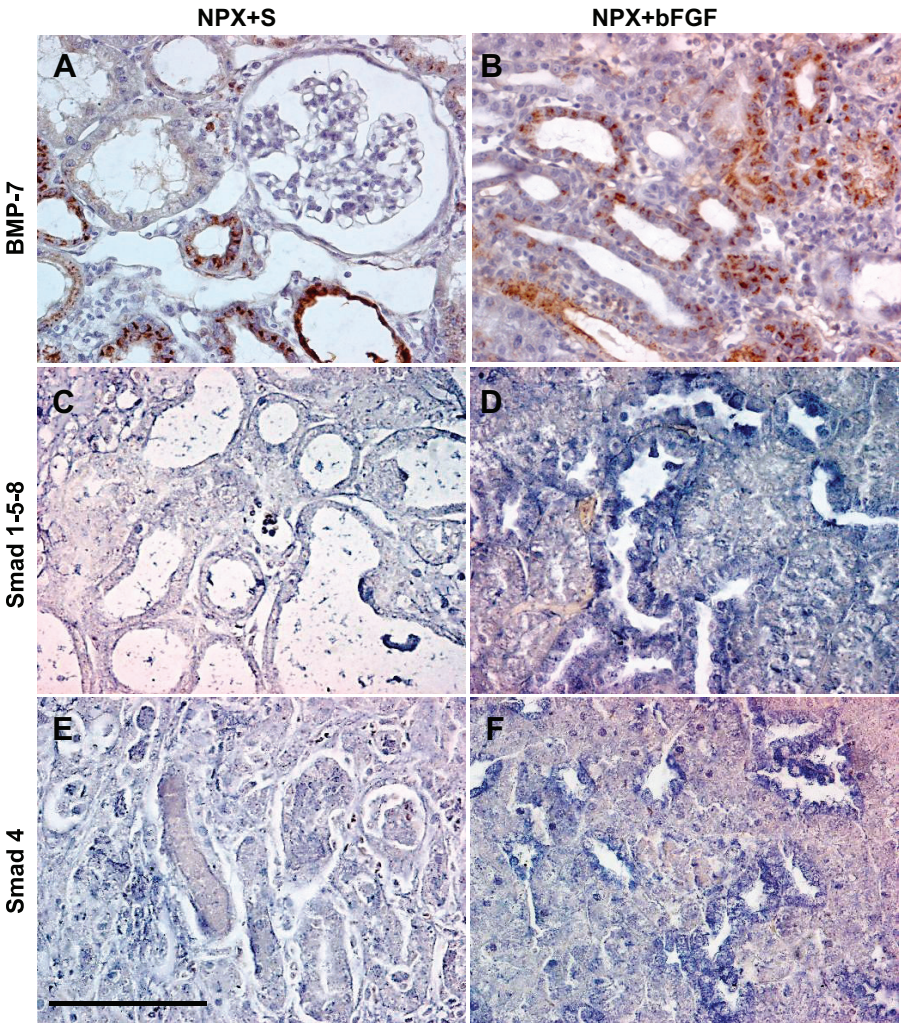

Fig. 8. Immunolocalization of the surviving factor BMP-7 and proteins from its transduction pathway. Samples were stained for BMP-7 (*A* and *B*), Smads 1-5-8 (*C* and *D*), and Smad 4 (*E* and *F*) 35 days after NPX and injection with bFGF (*B*, *D*, and *F*) or saline (*A*, *C*, and *E*). Kidneys NPX-treated with saline (*A*, *C*, and *E*) show lighter staining compared with kidneys NPX-injected with bFGF (*B*, *D*, and *F*), which showed marked intensity in staining. For BMP-7, staining was performed using DAB (brown reaction); for Smads 1-5-8 and Smad 4, staining was performed using NBT:BCIP (blue reaction). Scale bar = 100 μm.

higher quantities of functional glomeruli and tubular cells. In orchestration, these effects can contribute to decreasing the work overload of the remaining nephrons, thus allowing the kidneys to function better.

A transcription factor induced by hypoxia is HIF-1α (29). This factor is widely expressed in damaged tissue, including that found in ARF (40), and has a protective role in ischemic kidney events. HIF-1α induction is an early event in the sequence of cellular changes following the interruption of blood flow (29). It is likely to play an important role in subsequent reactions. The upregulation of HIF-1α has been involved in cell survival by inducing the angiogenic proteins VEGF and Tie-2 (7). Additionally, the overexpression of HIF-1α has been reported in CKD (16).

In the present study, we observed that HIF-1α levels are higher when bFGF is exogenously added, despite the fact that kidneys were submitted to the same hypoxic event in both groups of animals. This suggests that bFGF could be participating in the regulation of HIF-1α expression, as previously reported (44). Because we found HIF-1α expression in areas that also express angiogenic and epitheliogenic proteins, it is possible that HIF-1α may play an important role in cell death or survival decisions, hence inducing the cell to express morphogenic proteins. It is possible that the early presence of bFGF could harness the effects induced by HIF-1α.

CKD has been tightly linked to tubular epithelial cell injury. However, important vascular elements are also involved, due to the damage induced in peritubular capillaries (32). Considering these data, we analyzed the expression of the angiogenic factors VEGF and Tie-2. VEGF is essential for endothelial cell differentiation (i.e., vasculogenesis) and the sprouting of new capillaries from preexisting vessels (i.e., angiogenesis). Evidence has shown that VEGF is a factor that allows for the survival and proliferation of different cell types under extreme stress conditions (22). In addition, the upregulation of VEGF by bFGF has been previously reported (36). Another protein involved in kidney repair is the angiopoietin receptor Tie-2, since it plays an important role in the stabilization of vascular integrity (35). In our study, bFGF induced higher expression levels of VEGF and Tie-2, suggesting a protective role, probably mediated by maintaining glomerular filtration barrier integrity in CKD.

In different damage conditions, adult renal cells have the capacity to reexpress some proteins that are originally found during kidney development. This is a phenomenon considered by some to be essential in renal recovery (48, 49). Examples of these proteins are Pax-2, bFGF, Ncam, BMP-7, Lim-1, and Wnt-4 (19). The results obtained in this study using a CKD model treated with bFGF are in accordance with data published recently regarding ARF, where reexpression of these factors

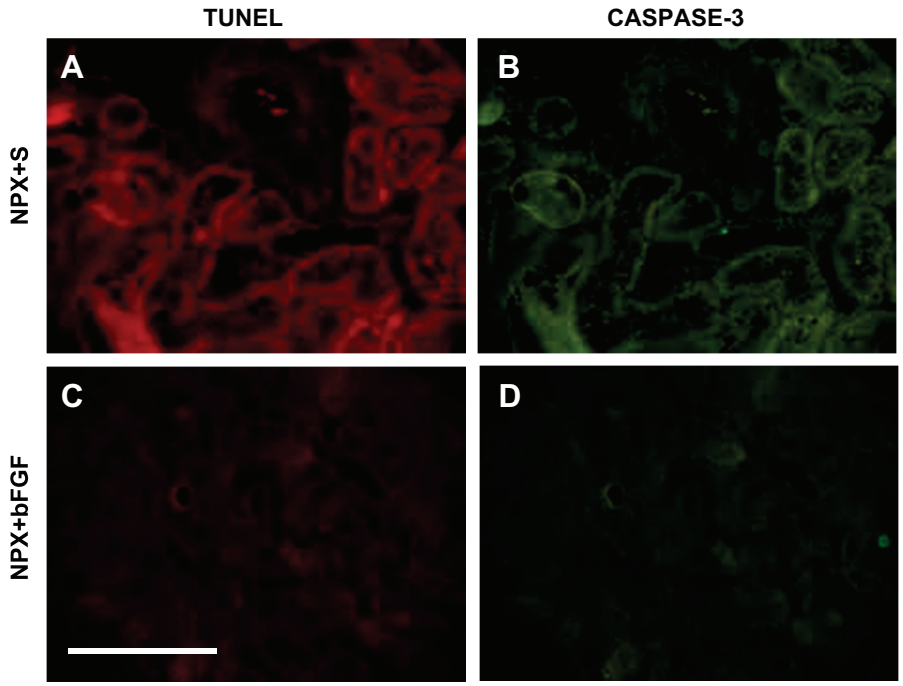

Fig. 9. Distribution of terminal transferase-dUTP-nick-end labeling (TUNEL) and caspase-3-positive cells in hypoxia induced by ischemia-reperfusion (I/R). TUNEL techniques (*A* and *C*) and immunohistochemistry for caspase-3 (*B* and *D*) were performed in kidney samples obtained 35 days after nephrectomy of animals injected with saline (*A* and *B*) or bFGF (*C* and *D*); $n = 5$/NPX group. Clear staining localized proximal to tubular cells from the inner and outer medulla area was observed in kidneys injected with saline (*A* and *B*), which was diminished in kidneys injected with bFGF (*C* and *D*). Staining for TUNEL and caspase-3 was done using fluorescence (Texas red and green color reaction, respectively). Scale bar = 100 μm.

was observed in direct relation to renal recovery (48, 49). This observation supports the theory that adult renal cells might have the capacity to reexpress specific repairing proteins when treated with bFGF as a particular morphogen. The deceleration of the progression of the disease observed in this study, as observed based on relative decreases in structural and functional damage, can also be explained due to the fact that bFGF stimulates renal cells to render a nephrogenic process (28). This induces an embryological environment, allowing the cells to dedifferentiate into mesenchymal states, thus reex-

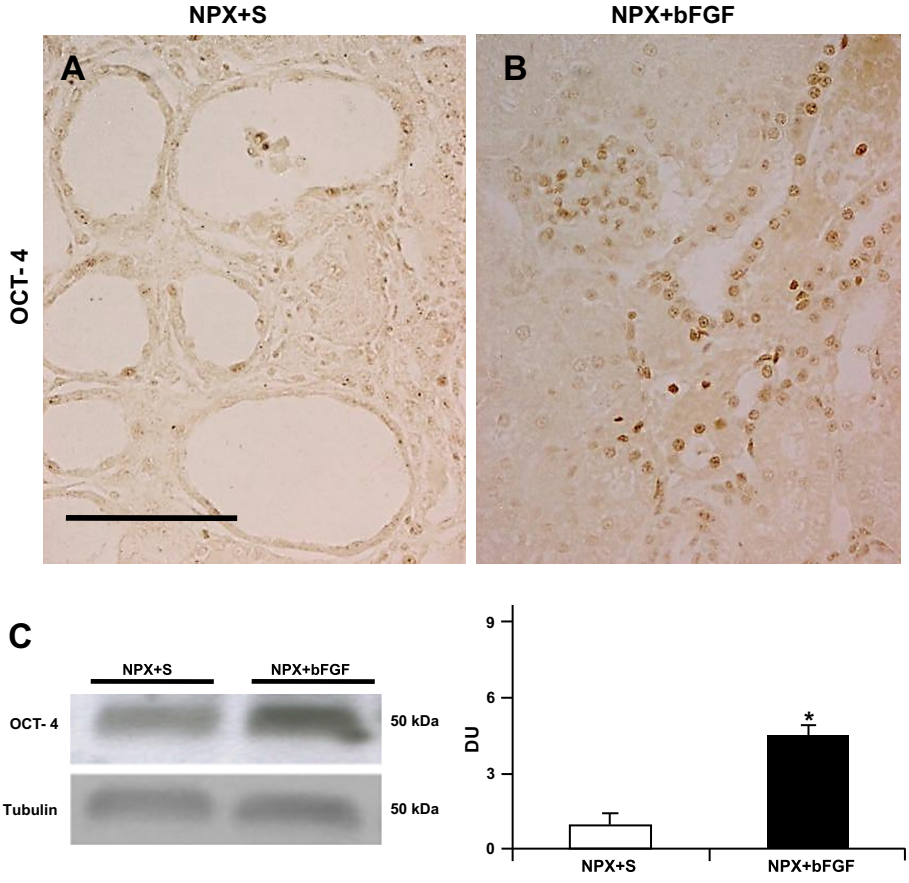

Fig. 10. Renal stem cells (SCs): expression and localization. The presence of renal SCs was evaluated by using the Oct-4 marker. Oct-4 localization was evaluated by immunohistochemistry in kidney samples 35 days after nephrectomy and saline (*A*) or bFGF injection (*B*). Induction of Oct-4 staining was observed in NPX+bFGF kidneys (*B*), which was not observed in NPX+S animals (*A*). Scale bar = 100 μm. Immunoblot (*C*) shows increased expression of Oct-4 in animals injected with bFGF compared with respective saline controls. $*P < 0.05$.

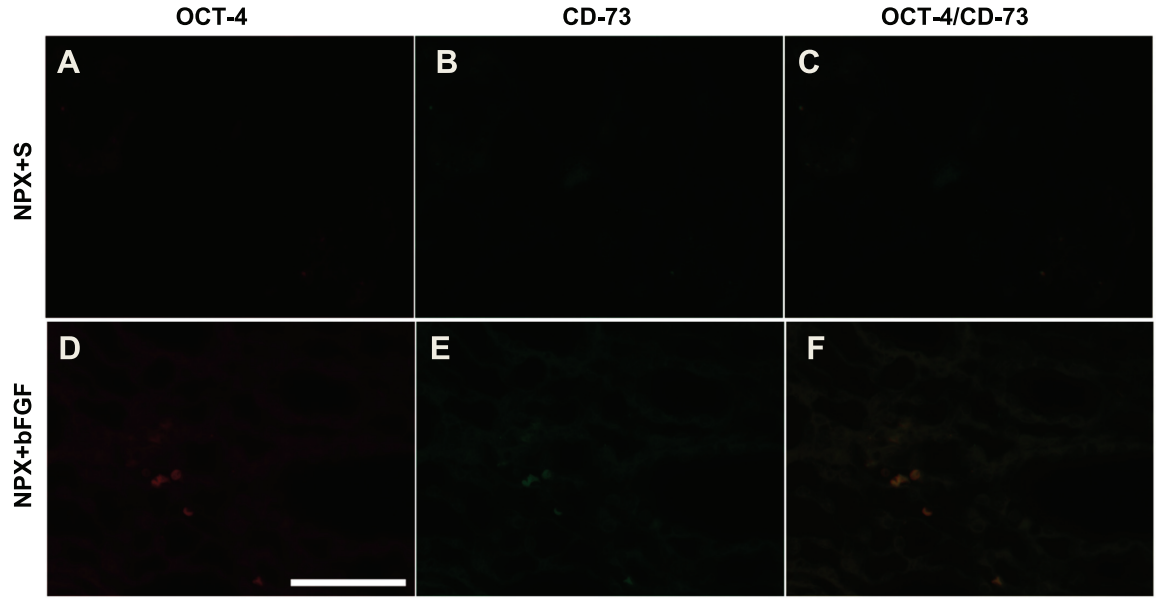

Fig. 11. Colocalization of CD73/OCT4. CD73 (*A* and *D*) and Oct-4 (*B* and *E*) were observed in kidney sections 35 days after bFGF injection (*D* and *E*). The *right* panels (*C* and *F*) correspond to merge microscope techniques. Scale bar = 100 μm.

pressing the factors needed for regeneration (48). A recent paper has suggested that Wnt-4 may be involved in the progression of renal fibrosis (10) instead of repair. We believe that the differences between that observation and ours can be attributed to the animal models used (mouse vs. rat, and transgenic vs. naive). In addition, timing and amount are two variables to be considered. In the repair process, morphogen levels are lower than in the state of chronic induction. These lower levels for a shorter period of time can stimulate renal cells to enter a proliferative stage and induce a microenvironment similar to the one described for embryonic kidney development limited in time. In contrast, morphogens can induce unregulated increases in myofibroblasts and fibrosis in a state of chronic induction. Additional studies are necessary to fill such gaps.

The BMP signaling pathway is mediated by Smad proteins in kidney development (53). The spatial and temporal expression patterns of Smads have been described in mesenchymal cells of the nephrogenic zone during kidney development (53), where Smads are downregulated once these cells begin to epithelialize. We observed Smads 1-5-8 (activated by BMP) and Smad 4 (a coactivator and mediator of signal transduction) being reexpressed after damage in kidneys treated with bFGF. The latter, together with the presence of nephrogenic proteins and the highest levels of Noggin and BMP, are in accordance to what has been reported previously (48). Based on the observed patterns of expression, we speculate that one member of the Smad family, or a combination of more than one member, could play specific roles in regeneration during kidney damage and be involved in the nephrogenic process, thus repeating what takes place during kidney development.

The results obtained in this study regarding the effects of bFGF on renal injury are particularly important, because they add to previous reports that have shown beneficial roles for bFGF in the recovery from acute renal damage (48). It has been suggested that bFGF can induce a number of tubulogenic/epitheliogenic and angiogenic proteins, which in turn will be responsible for kidney regeneration (47, 48). Additionally, it was proposed that the short-term injury produced in acute damage could be an advantageous stimulus to the induction of repairing proteins, and bFGF only enhanced this process (48). These findings in CKD open the possibility that bFGF not only induces repairing proteins but also could be involved in maintaining a continuous effect on these proteins during injury (acute or chronic), allowing the kidneys to recover. A possibility that was not explored is this study is that bFGF was injected when the initial damaged occurred by nephrectomy. This could be considered to constitute acute damage at this stage. In this context, bFGF could only stop the damage progression, instead of allowing regeneration. Additional studies are necessary to respond to this question.

In uremic rats, a mild but significant increase in the renal SC marker Oct-4 (17) has been demonstrated after the injection of mesenchymal SC. This observation is consistent with our results regarding the reexpression of Oct-4 and could be explained in at least two ways. First, an induction of tubular and epithelial cells might take place to drive epithelial tissue to mesenchymal transition processes. Then, these mesenchymal cells could proliferate and differentiate, resulting in renal reparative phenomenon. Alternatively, Oct-4-positive cells could just be resident kidney SC, which under appropriate stimulation would proliferate and mediate kidney repair. In this regard, we must emphasize that these two pathways are not mutually exclusive, and that they both probably play a role in tissue regeneration. Further studies are needed to address this issue.

In conclusion, our results suggest that bFGF reduces the functional and morphological damage involved in CKD and induces the reexpression of nephrogenic/angiogenic factors and Oct-4, which are characteristic of embryological kidney development. This study opens new perspectives for future research on treatments, where the use of growth factors could reduce functional and structural damage in CKD.

ACKNOWLEDGMENTS

The authors thank María Alcoholado and José M. Erpel for technical assistance in tissue processing and Christian Lührs Undurraga for critical reading of the manuscript.

GRANTS

This work was supported by Fondecyt Grant 11075029 (S. Villanueva), 1130741 (C. P. Vio), FAI 002-08 (S. Villanueva, C. P. Vio), and the Programa de Financiamiento Basal PFB 12-2007, SQM (C. P. Vio).

DISCLOSURES

No conflicts of interest, financial or otherwise, are declared by the authors.

AUTHOR CONTRIBUTIONS

Author contributions: S.V. and J.E.C. provided conception and design of research; S.V., A.T., J.E.C., C.V., E.E., C.C., C.I., M.S., V.V., and C.P.V. analyzed data; S.V., F.C., J.E.C., C.V., E.E., C.I., M.S., and V.V. interpreted results of experiments; S.V., A.T., J.E.C., C.V., E.E., C.C., C.I., V.V., and C.P.V. drafted manuscript; S.V., J.E.C., C.I., V.V., and C.P.V. edited and revised manuscript; S.V., J.E.C., V.V., and C.P.V. approved final version of manuscript; F.C., A.T., C.V., E.E., C.C., and M.S. performed experiments; F.C., A.T., C.V., and C.C. prepared figures.

REFERENCES

1. **Abbate M, Brown D, Bonventre J.** Expression of NCAM recapitulates tubulogenic development in kidneys recovering from acute ischemia. *Am J Physiol Renal Physiol* 277: F454–F463, 1999.
2. **Barasch J, Qiao J, McWilliams G, Chen D, Oliver JA, Herzlinger D.** Ureteric bud cells secrete multiple factors, including bFGF, which rescue renal progenitors from apoptosis. *Am J Physiol Renal Physiol* 273: F757–F767, 1997.
3. **Bellomo R, Ronco C, Kellum JA, Mehta RL, Palevsky P, Acute Dialysis Quality Initiative Workgroup.** Acute renal failure—definition, outcome measures, animal models, fluid therapy and information technology needs: the Second International Consensus Conference of the Acute Dialysis Quality Initiative (ADQI) Group. *Crit Care* 8: R204–R212, 2004.
4. **Breier G, Albrecht U, Sterrer S, Risau W.** Expression of vascular endothelial growth factor during embryonic angiogenesis and endothelial cell differentiation. *Development* 114: 521–532, 1992.
5. **Brunet LJ, McMahon JA, McMahon AP, Harland RM.** Noggin, cartilage morphogenesis, and joint formation in the mammalian skeleton. *Science* 280: 1455–1457, 1998.
6. **Cai Q, Dmitrieva N, Ferraris J, Brooks H, van Balkom B, Burg M.** Pax2 expression occurs in renal medullary epithelial cells in vivo and in cell culture, is osmoregulated, and promotes osmotic tolerance. *Proc Natl Acad Sci USA* 102: 503–508, 2005.
7. **Chen L, Endler A, Shibasaki F.** Hypoxia and angiogenesis: regulation of hypoxia-inducible factors via novel binding factors. *Exp Mol Med* 41: 849–857, 2009.
8. **Colleoni S, Bottani E, Tessaro I, Mari G, Merlo B, Romagnoli N, Spadari A, Galli C, Lazzari G.** Isolation, growth and differentiation of equine mesenchymal stem cells: effect of donor, source, amount of tissue and supplementation with basic fibroblast growth factor. *Vet Res Commun* 33: 811–821, 2009.
9. **Coresh J, Byrd-Holt D, Astor BC, Briggs JP, Eggers PW, Lacher DA, Hostetter TH.** Chronic kidney disease awareness, prevalence and trends among US adults, 1999 to 2000. *J Am Soc Nephrol* 16: 180–188, 2005.
10. **DiRocco DP, Kobayashi A, Taketo MM, McMahon AP, Humphreys BD.** Wnt4/β-catenin signaling in medullary kidney myofibroblasts. *JASN* 24: 1399–1412, 2013.
11. **Dudley AT, Godin RE, Robertson EJ.** Interaction between FGF and BMP signaling pathways regulates development of metanephric mesenchyme. *Genes Dev* 13: 1601–1613, 1999.
12. **Dudley AT, Lyons KM, Robertson EJ.** A requirement for bone morphogenetic protein-7 during development of the mammalian kidney and eye. *Genes Dev* 9: 2795–2807, 1995.
13. **Fleck C, Appenroth D, Jonas P, Koch M, Kundt G, Nizze H, Stein G.** Suitability of 5/6 nephrectomy (5/6NX) for the induction of interstitial renal fibrosis in rats—influence of sex, strain, and surgical procedure. *Exp Toxicol Pathol* 57: 195–205, 2006.
14. **Galle J.** Reduction of proteinuria with angiotensin receptor blockers. *Nat Clin Pract Cardiovasc Med* 5: S36–S43, 2008.
15. **Goda N, Dozier SJ, Johnson RS.** HIF-1 in cell cycle regulation, apoptosis, and tumor progression. *Antioxid Redox Signal* 5: 467–473, 2003.
16. **Gunaratnam L, Bonventre JV.** HIF in kidney disease and development. *J Am Soc Nephrol* 20: 1877–1887, 2009.
17. **Gupta S, Verfaillie C, Chmielewski D, Kren S, Eidman K, Connaire J, Heremans Y, Lund T, Blackstad M, Jiang Y, Luttun A, Rosenberg ME.** Isolation and characterization of kidney-derived stem cells. *J Am Soc Nephrol* 17: 3028–3040, 2006.
19. **Imgrund M, Grone E, Grone HJ, Kretzler M, Holzman L, Schlondorff D, Rothenpieler UW.** Re-expression of the developmental gene Pax-2 during experimental acute tubular necrosis in mice. *Kidney Int* 56: 1423–1431, 1999.
20. **Karanova I, Dove L, Resau J, Perantoni A.** Conditioned medium from a rat ureteric bud cell line in combination with bFGF induces complete differentiation of isolated metanephric mesenchyme. *Development* 122: 4159–4167, 1996.

21a. **Kaspar DL, Braunwald E, Hauser S, Longo D, Jameson JL, Fauci AS, Editors.** *Harrison Principios de Medicina Interna*. New York: McGraw-Hill, 2007.

21. **Kelly DJ, Hepper C, Wu LL, Cox AJ, Gilbert RE.** Vascular endothelial growth factor expression and glomerular endothelial cell loss in the remnant kidney model. *Nephrol Dial Transplant* 18: 1286–1292, 2003.
22. **Kim BS, Goligorsky MS.** Role of VEGF in kidney development, microvascular maintenance and pathophysiology of renal disease. *Korean J Intern Med* 18: 65–75, 2003.
23. **Kolatsi-Joannou M, Li XZ, Suda T, Yuan IT, Woolf AS.** Expression and potential role of angiopoietins and Tie-2 in early development of the mouse metanephros. *Dev Dyn* 222: 120–126, 2001.
24. **Kopp JB.** BMP receptors in kidney. *Kidney Int* 58: 2237–2238, 2000.
25. **Lackie PM, Zuber C, Roth J.** Polysialic acid and N-CAM localisation in embryonic rat kidney: mesenchymal and epithelial elements show different patterns of expression. *Development* 110: 933–947, 1990.
26. **Lazarous DF, Unger EF, Epstein SE, Stine A, Arevalo JL, Chew EY, Quyyumi AA.** Basic fibroblast growth factor in patients with intermittent claudication: results of a phase I trial. *J Am Coll Cardiol* 36: 1239–1244, 2000.
27. **Lederman RJ, Mendelsohn FO, Anderson RD, Saucedo JF, Tenaglia AN, Hermiller JB, Hillegass WB, Rocha-Singh K, Moon TE, Whitehouse MJ, Annex BH.** Therapeutic angiogenesis with recombinant fibroblast growth factor-2 for intermittent claudication (the TRAFFIC study): a randomised trial. *Lancet* 359: 2053–2058, 2002.
28. **Lemiere S, Azar R, Belloc F, Gürsel D, Pyronnet S, Bikfalvi A, Auguste P.** Overexpression of high molecular weight FGF-2 forms inhibits glioma growth by acting on cell-cycle progression and protein translation. *Exp Cell Res* 314: 3701–3711, 2008.
29. **Manotham K, Tanaka T, Ohse T, Kojima I, Miyata T, Inagi R, Tanaka H, Sassa R, Fujita T, Nangaku M.** A biologic role of HIF-1 in the renal medulla. *Kidney Int* 67: 1428–1439, 2005.
30. **Miyamoto K, Kitamoto Y, Tokunaga H, Takeya M, Ezaki T, Imamura T, Tomita K.** Protective effect of vascular endothelial growth factor/vascular permeability factor 165 and 121 on glomerular endothelial cell injury in the rat. *Lab Invest* 84: 1126–1136, 2004.
31. **Naito T, Ma LJ, Yang H, Zuo Y, Tang Y, Han JY, Kon V, Fogo AB.** Angiotensin type 2 receptor actions contribute to angiotensin type 1 receptor blocker effects on kidney fibrosis. *Am J Physiol Renal Physiol* 298: F683–F691, 2010.
32. **Nangaku M.** Mechanisms of tubulointerstitial injury in the kidney: final common pathways to end-stage renal failure. *Intern Med* 43: 9–17, 2004.
33. **Navaneethan SD, Nigwekar SU, Sehgal AR, Strippoli GF.** Aldosterone antagonists for preventing the progression of chronic kidney disease: a systematic review and meta-analysis. *Clin J Am Soc Nephrol* 4: 542–551, 2009.
34. **Pedersen A, Skjong C, Shawlot W.** Lim 1 is required for nephric duct extension and ureteric bud morphogenesis. *Dev Biol* 288: 571–581, 2005.
35. **Pitera JE, Woolf AS, Gale NW, Yancopoulos GD, Yuan HT.** Dysmorphogenesis of kidney cortical peritubular capillaries in angiopoietin-2-deficient mice. *Am J Pathol* 165: 1895–1906, 2004.
36. **Rabie AB, Lu M.** Basic fibroblast growth factor up-regulates the expression of vascular endothelial growth factor during healing of allogeneic bone graft. *Arch Oral Biol* 49: 1025–1033, 2004.
37. **Rieck PW, Gigon F, M, Jaroszewski J, Pleyer U, Hartmann C.** Increased endothelial survival of organ-cultured corneas stored in FGF-2-

supplemented serum-free medium. *Invest Ophtalmol Vis Sci* 44: 3826–3832, 2003.
38. **Ripley E.** Complementary effects of angiotensin-converting enzyme inhibitors and angiotensin receptor blockers in slowing the progression of chronic kidney disease. *Am Heart J* 157: S7–S10, 2009.
39. **Rogelj S, Klagsbrun M, Atzmon R, Kurokawa M, Haimovitz A, Fuks Z, Vlodavsky I.** Basic fibroblast growth factor is an extracellular matrix component required for supporting the proliferation of vascular endothelial cells and the differentiation of PC 12 cells. *J Cell Biol* 109: 823–831, 1989.
40. **Rosenberger C, Mandriota S, Jurgensen JS, Wiesener MS, Horstrup JH, Frei U, Ratcliffe PJ, Maxwell PH, Bachmann S, Eckardt KU.** Expression of hypoxia-inducible factor-1alpha and -2alpha in hypoxic and ischemic rat kidneys. *J Am Soc Nephrol* 13: 1721–1732, 2002.
41. **Rothenpieler UW, Dressler GR.** Pax-2 is required for mesenchyme-to-epithelium conversion during kidney development. *Development* 119: 711–720, 1993.
42. **Saksela O, Moscatelli D, Sommer A, Rifkin DB.** Endothelial cell-derived heparan sulfate binds basic fibroblast growth factor and protects it from proteolytic degradation. *J Cell Biol* 107: 743–751, 1998.
43. **Sengul E, Sahin T, Sevin E, Yilmaz A.** Effect of spironolactone on urinary protein excretion in patients with chronic kidney disease. *Ren Fail* 31: 928–932, 2009.
44. **Shi YH, Bingle L, Gong LH, Wang YX, Corke KP, Fang WG.** Basic FGF augments hypoxia induced HIF-1alpha expression and VEGF release in T47D breast cancer cells. *Pathology* 39: 396–400, 2007.
45. **Singri N, Ahya SN, Levin ML.** Acute renal failure. *JAMA* 289: 747–751, 2003.
46. **Unger EF, Goncalves L, Epstein SE, Chew EY, Trapnell CB, Cannon RO 3rd, Quyyumi AA.** Effects of a single intracoronary injection of basic fibroblast growth factor in stable angina pectoris. *Am J Cardiol* 85: 1414–1419, 2000.
47. **Villanueva S, Cespedes C, Gonzalez AA, Roessler E, Vio CP.** Inhibition of bFGF-receptor type 2 increases kidney damage and suppresses nephrogenic protein expression after ischemic acute renal failure. *Am J Physiol Regul Integr Comp Physiol* 294: R819–R828, 2008.
48. **Villanueva S, Cespedes C, González A, Vio CP.** bFGF induces an earlier expression of nephrogenic proteins after ischemic acute renal failure. *Am J Physiol Regul Integr Comp Physiol* 291: R1677–R1687, 2006.
49. **Villanueva S, Cespedes C, Vio CP.** Ischemic acute renal failure induces the expression of a wide range of nephrogenic proteins. *Am J Physiol Regul Integr Comp Physiol* 290: R861–R870, 2006.
50. **Villanueva S, Glavic A, Ruiz P, Mayor R.** Posteriorization by FGF, Wnt and retinoic acid is required for neural crest induction. *Dev Biol* 241: 289–301, 2002.
51. **Vio CP, An SJ, Cespedes C, McGiff JC, Ferreri NR.** Induction of cyclooxygenase-2 in thick ascending limb cells by adrenalectomy. *J Am Soc Nephrol* 12: 649–658, 2001.
52. **Vio CP, Cespedes C, Gallardo P, Masferrer JL.** Renal identification of cyclooxygenase-2 in a subset of thick ascending limb cells. *Hypertension* 30: 687–692, 1997.
53. **Vrljicak P, Myburgh D, Ryan AK, Van Rooijen MA, Mummery CL, Gupta IR.** Smad expression during kidney development. *Am J Physiol Renal Physiol* 286: F625–F633, 2004.
54. **Wagner KD, Wagner N, Wellmann S, Schley G, Bondke A, Theres H, Scholz H.** Oxygen-regulated expression of the Wilms tumor suppressor *Wt1* involves hypoxia-inducible factor-1 (HIF-1). *FASEB J* 171: 364–1366, 2003.
55. **Witzgall R, Brown D, Schwarz C, Bonventre JV.** Localization of proliferating cell nuclear antigen, vimentin, c-Fos, and clusterin in the postischemic kidney. Evidence for a heterogeneous genetic response among nephron segments, and a large pool of mitotically active and dedifferentiated cells. *J Clin Invest* 93: 2175–2188, 1994.